Periodic Alignment of Binary Droplets via a Microphase Separation of a Tripolymer Solution under Tubular Confinement

Mayu Shono, Koki Aburatani, Miho Yanagisawa, Kenichi Yoshikawa, and Akihisa Shioi*

Read Online
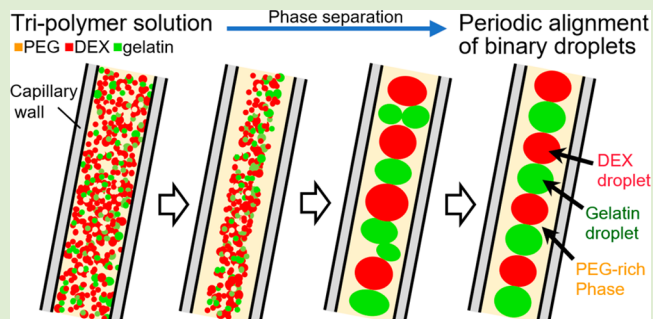
| ACCESS | | Metrics & More | | Article Recommendations | | Supporting Information |

ABSTRACT: We report the spontaneous formation of a characteristic periodic pattern through the phase separation of a tripolymer solution comprising polyethylene-glycol (PEG)/dextran (DEX)/gelatin. When this tripolymer solution is introduced into a glass capillary with a PEG-coated inner surface, we observe the time-dependent growth of microphase separation. Remarkably, a self-organized, periodic alignment of DEX- and gelatin-rich microdroplets ensues, surrounded by a PEG-rich phase. This pattern demonstrates considerable stability, enduring for at least 8 h. The fundamental characteristics of the experimentally observed periodic alignment are successfully replicated via numerical simulations using a Cahn−Hilliard model underpinned by a set of simple, theoretically derived equations. We propose that this type of kinetically stabilized periodic patterning can be produced across a broad range of phase-separation systems by selecting appropriate boundary conditions such as at the surface within a narrow channel.

Research into the spatial patterns arising from phase transitions and aggregations in polymer systems has been vigorously pursued from both theoretical and experimental perspectives.[1−19] Commonly, in first-order phase transitions,[7−10] excluding critical phenomena, such as spinodal decomposition[11−15] and nucleation and growth,[16−18] the spatial scale of the pattern tends to increase, or coarsen, over time. Consequently, transient microscopic patterns evolve during phase separation. To halt the coarsening and capture the pattern at a microscopic scale, a rapid decrease in temperature is often employed.[20−23] However, this approach typically results in a disordered microstructure, as observed in glass transitions,[24−30] for example. Conversely, our recent findings reveal the spontaneous alignment of uniformly sized microdroplets within a quasi-one-dimensional confinement (quasi-1D). This pattern, emerging from the phase separation of two types of hydrophilic polymers in water within a capillary, organizes itself.[31,32] In this present study, we demonstrate that a periodic alignment of binary microdroplets, each surrounded by a different polymer solution, arises from the phase separation of an aqueous tripolymer solution in a capillary. Recently, in the studies concerning coacervate formation, generation of various specific spatial patterns with polydispersity have been reported.[19,33−38] It is particularly notable that the periodic pattern formation of our study occurs in a thermodynamically closed system, which is in contrast to the pattern formation observed in thermodynamically open systems, such as the reaction-diffusion system responsible for Turing patterns.[39−42] In essence, the spatial periodic pattern in

our system is kinetically stable, persisting without the need for a continuous input of energy or materials, distinguishing it from the dynamics of patterning in reaction-diffusion systems.

Polyethylene-glycol (PEG) with an average molecular weight (MW) of 6000, dextran (DEX, MW: 200,000), and gelatin were purchased from Fujifilm Wako Pure Chemical Industries (Osaka, Japan). Three types of solutions with different compositions were prepared by mixing the polymers with fully deionized water. The compositions were (i) 4.2 wt % (PEG)/3.3 wt % (DEX)/5.0 wt % (gelatin), (ii) 3.9 wt %/3.1 wt %/4.7 wt %, and (iii) 3.6 wt %/2.9 wt %/4.3 wt %. We thus chose the fixed relative compositions of PEG/DEX/gelatin with a ratio of 5:4:6 in weight. In these compositions of (i)−(iii), we confirmed that macroscopic phase separation with three different phases is generated in the bulk for the mechanically mixed solution. It has been reported that phase separation occurs between each polymeric pair in the tripolymers.[43−46] For fluorescence observation, DEX and gelatin were labeled with TRITC-dextran (excitation wavelength [Ex]: 550 nm; emission wavelength [Em]: 572 nm; TdB Laboratories AB, Uppsala, Sweden) and FITC-I
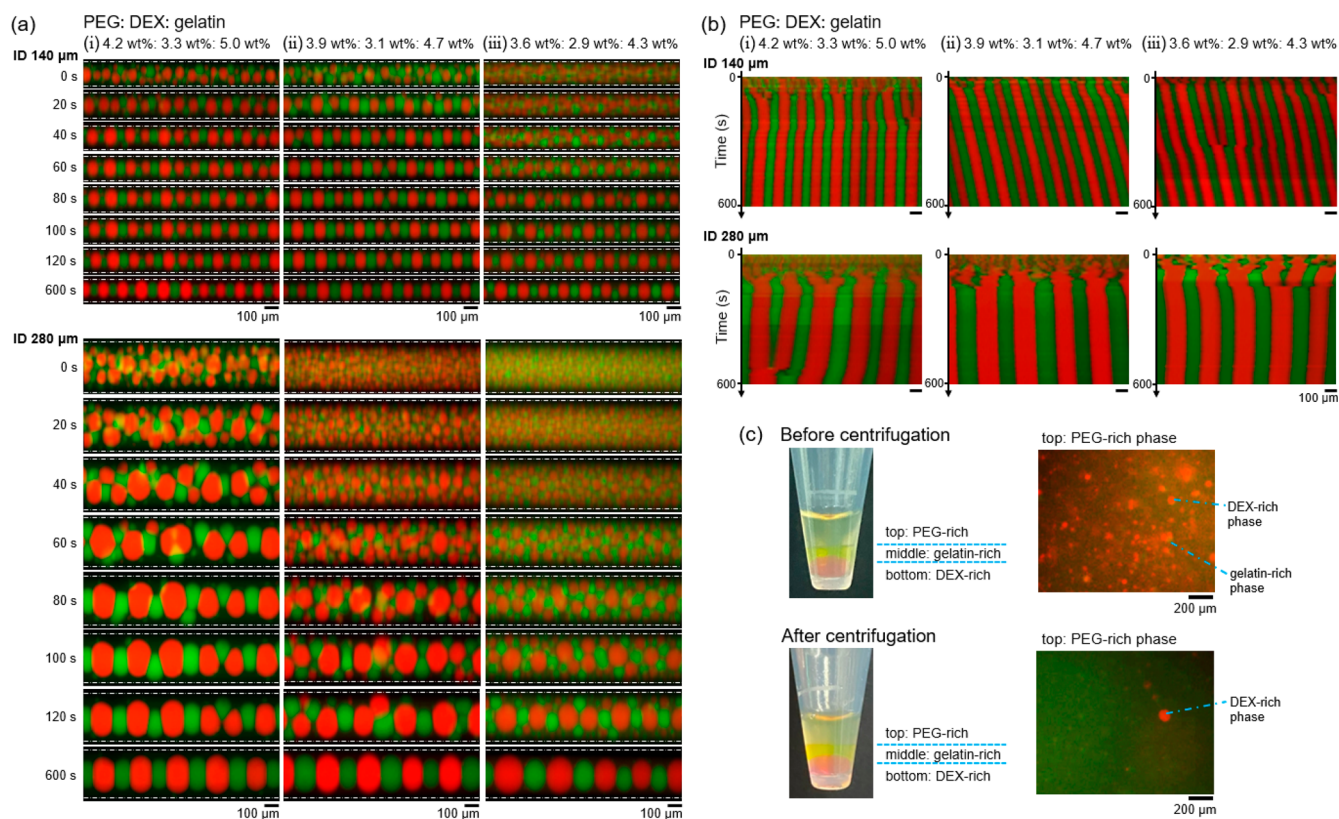
Figure 1. Spontaneous pattern formation in a three-phase system (PEG+DEX+gelatin) within a PEG-coated glass capillary. The compositions of the PEG/DEX/gelatin are (i) 4.2 wt %/3.3 wt %/5.0 wt %; (ii) 3.9 wt %/3.1 wt %/4.7 wt %; (iii) 3.6 wt %/2.9 wt %/4.3 wt %. The red, green, and black (no fluorescence) regions correspond to the DEX- (labeled with TRITC-dextran), gelatin- (labeled with FITC-I) and PEG-rich phases, respectively. White dashed lines indicate the position of the inner glass wall. (a) Snapshots of the solution inside the capillary (inner diameter: 140 μm, 280 μm) at the different times. (b) Spatiotemporal plot of (a). (c) Macroscopic phase separation of the PEG/DEX/gelatin solution in bulk. The composition of the PEG/DEX/gelatin is 4.2 wt %/3.3 wt %/5.0 wt %. Upper: Before centrifugation (at 60 °C in the incubator and for 20 min after mixing the solution); Lower: After centrifugation for 1 min (3000 rpm). The top, middle, and bottom phases correspond to the PEG-, gelatin-, and DEX-rich phases, respectively. The right panels show the fluorescence microscopy of the top (PEG-rich) phase on the glass slide.

(fluorescein isothiocyanate isomer I; Ex: 488 nm; Em: 530 nm; Sigma-Aldrich, St. Louis, MO, U.S.A.), respectively. A glass capillary (Microcaps; Drummond, U.S.A.) with an inner diameter of 140 or 280 μm and 32 mm in the long axis was used. For PEG-coating of the inner wall of the capillary, poly-L-lysine(20) graft[3,5] PEG(2) (PLL(20)-g[3,5]-PEG(2); SuSoS AG, Switzerland) was used according to the reported method.[32]

The three types of solution ((i), (ii), and (iii)) were incubated at 60 °C and mixed further using a vortex mixer until they looked cloudy. The solution thus mixed by mechanical stirring was then sucked up into the PEG-coated capillary. Both ends of the capillary were sealed to avoid leakage and evaporation of the solution. For fluorescence microscopy (Olympus IX71; Olympus Co., Tokyo, Japan), the capillaries were maintained horizontally on a heat stage (TPi-CKTS; Tokai hit, Shizuoka, Japan) at 60 °C. The images were obtained with a complementary metal oxide semiconductor (CMOS) digital camera (DP74; Olympus Co., Tokyo, Japan). For centrifugation, Sigma 1−14 (SGM10015; Sigma, Kanagawa, Japan) was used.

Figure 1a illustrates the progression of phase separation within the PEG-coated capillary, which shows a preferential attraction of the PEG-rich phase to the surface over the other polymers. The times listed represent the duration elapsed since the commencement of microscopy observation, which occurs

approximately 60 s after phase separation begins. The red, green, and black (no fluorescence) areas denote the DEX-, gelatin-, and PEG-rich phases, respectively. In the case of a capillary with an inner diameter of 140 μm and composition (i), the PEG-rich phase moistened the inner wall in the very initial stage (0 s). At this juncture, the DEX/gelatin phases, being repelled from the inner wall, underwent phase separation to form droplets that increased in size. The linear arrangement of the DEX-rich droplets started to take shape before that of the gelatin-rich droplets (at 40 s). The gelatin-rich droplets expanded, and a periodic alignment of DEX- and gelatin-rich droplets within the PEG-rich solution spontaneously established itself (120 s). Although the rate of pattern formation varied depending on the capillary diameter and the mixture's composition, the ultimate pattern remained consistent: patterns across different capillary diameters shared a similarity when scaled by diameter, and pattern formation occurred more swiftly in narrower capillaries. Figure 1b presents a spatiotemporal plot derived from images taken along a horizontal line bisecting the center of the capillary (as shown in Figure 1a). These plots confirm the generated pattern's stability for 10 min. The experimental results for longer time periods are shown in Figure S1 (Supporting Information), indicating that the periodic structure is maintained for 8 h after formation and changed somewhat at 24 h. A slight drift in droplet position was observed, likely due to a mild flow within

the capillary. Figure 1c illustrates the macroscopic phase separation in a bulk solution before (top) and after (lower) centrifugation. The composition of the PEG/DEX/gelatin is 4.2 wt % PEG, 3.3 wt % DEX, and 5.0 wt % gelatin, which corresponds to composition (i) in Figure 1a. The top, middle, and bottom phases correspond to the PEG-, gelatin-, and DEX-rich phases, respectively. The right panels of Figures 1c show the fluorescence microscopy of the top (PEG-rich) phase observed on the glass slide. The solution without centrifugation is incompletely divided into three phases at 20 min after mixing the solution. In the upper microscopic image, the DEX- and gelatin-rich droplets remained in the PEG-rich phase. After centrifugation for 1 min (3000 rpm), the macroscopic phase separation is clearly observed. In the lower microscopic image, the number of DEX-rich droplets was reduced. The pattern formed by the phase separation in bulk differs from those observed in Figure 1a.

Figure 2 shows the comparison in the pattern formation between the PEG/DEX/gelatin (three)- and the PEG/DEX
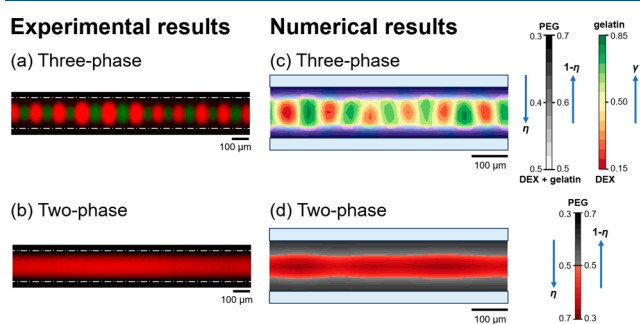
Figure 2. Pattern formation through the phase separation of the three- (PEG+DEX+gelatin) and two- (PEG+DEX) polymer solutions in the PEG-coated capillary (inner diameter: 140 μm). (a, b) Experimental results. The red, green, and black (no fluorescence) regions correspond to the DEX- (labeled with TRITC-dextran), gelatin- (labeled with FITC-I), and PEG-rich phases, respectively. The white dashed lines indicate the position of the inner glass wall. (a) The expanded image of Figure 1a-(i) at 600 s. (b) The two-phase separation (PEG/DEX = 4.2 wt %/3.3 wt %). (c, d) Numerical results on the pattern formation through the phase separation under quasi-one-dimensional confinement. The order parameters are represented as the color bar. The light blue area represents the capillary wall. (c) The three-phase (PEG/DEX/gelatin) separation (eqs 1−4). The calculation was sequential between PEG and DEX+gelatin and between DEX and gelatin. The black, red, and green regions corresponding to $\eta < 0.5$ (PEG-rich), $\gamma < 0.5$ (DEX-rich), and $\gamma > 0.5$ (gelatin-rich) phases, respectively. (d) The two-phase (PEG/DEX) separation (eqs 1 and 2). The black and red regions correspond to $\eta < 0.5$ (PEG-rich) and $\eta > 0.5$ (DEX-rich) phases, respectively.

(two)-polymer solution in a capillary (inner diameter: 140 μm). The compositions are (a) PEG/DEX/gelatin = 4.2 wt %/3.3 wt %/5.0 wt % corresponding to (i) and (b) PEG/DEX = 4.2 wt %/3.3 wt %. Figure 2a is the same as that in Figure 1a-(i) at 600 s. Figure 2b shows that the PEG-rich phase was attracted to the inner wall, and the cylindrical structure of the DEX-rich phase was generated in the center of the capillary via two-phase separation at 600 s.

Numerical modeling was performed to assess the generation mechanism of periodic pattern through the three- (PEG/DEX/gelatin) or two- (PEG/DEX) phase separation in capillary shown in Figure 2a,b. For the two-phase separation, the Cahn−Hilliard equation, eq 1, is applied as follows:

$$\frac{\partial \eta}{\partial t} = \nabla\left(M_c \nabla \frac{\delta F}{\delta \eta}\right) \tag{1}$$

where $M_c = (D_0/RT)$ is the diffusivity (F: free energy, t: time, D_0: diffusion constant). The relative ratio of DEX to the total PEG+DEX solution is represented as parameter η, where $\eta = [0, 1]$. $\eta = 0$ corresponds to the state without DEX. The free energy F can be expressed as

$$F = \int \left(RT[\eta \ln \eta + (1 - \eta)\ln(1 - \eta)] + L\eta(1 - \eta) + \frac{\alpha}{2}|\nabla \eta|^2 \right) dV \tag{2}$$

where L and α denote the parameters representing the interaction and interfacial energy between PEG and DEX phases, respectively (V: volume).

For the three-phase solution, one way to model three-phase solutions is to derive a Cahn−Hilliard-type equation by fitting the free energy functional of the three polymer components, but this suffers from a large number of tunable parameters. In this study, we carefully observed the phase separation dynamics (Figure 1a) and found that a PEG-rich phase appeared early near the glass surface, followed by phase separation between a DEX-rich phase and a gelatin-rich phase at the center of the glass tube. Based on this experimental result, we simulated the early and late stages of phase separation using eqs 1 and 2 and eqs 3 and 4, respectively. Using these equations greatly reduces the number of tunable parameters and makes it much easier to gain a basic understanding of the three-phase separation dynamics, as observed in this study. Therefore, the phase separation of three-solutions was divided into the two stages considering the results of Figure 1a, for the sake of simplicity, by avoiding the tentative parametrizations on many parameters in complicated equations. In the first stage, the phase separation between the PEG and DEX+gelatin phases was calculated using eqs 1 and 2 as if in the two-phase separation system. In this case, parameter η represents the relative ratio of DEX+gelatin to PEG+DEX+gelatin solution, where $\eta = [0, 1]$. For the second stage, let $\eta = \xi + (\eta - \xi)$ (ξ: DEX, $\eta - \xi$: gelatin) and $\gamma = \xi/\eta$. Equations 3 and 4 were used as extensions of eqs 1 and 2, respectively.

$$\frac{\partial \gamma}{\partial t} = \nabla\left(M_c' \nabla \frac{\delta F'}{\delta \gamma}\right) \tag{3}$$

where $M_c' = \eta^2(D_0/RT)$ denotes the diffusivity. Free energy F' can be expressed as follows:

$$F' = \int \left(RT[\gamma \ln \gamma + (1 - \gamma)\ln(1 - \gamma)] + L'\gamma(1 - \gamma) + \frac{\alpha'}{2}|\nabla \gamma|^2 \right) dV \tag{4}$$

Further numerical details with the boundary conditions and parameters are provided in the Supporting Information.

Figure 2c,d shows the numerical results corresponding to the time periods of 10 min. The order parameters are represented as the color bar. Figure 2c shows the calculation results of the three-phase separation using eqs 1−4. Furthermore, black, red, and green regions correspond to $\eta < 0.5$ (PEG-rich), $\gamma < 0.5$ (DEX-rich), and $\gamma > 0.5$ (gelatin-rich) phases, respectively. The periodic alignment of the DEX and gelatin phase surrounded by a PEG-rich solution is developed. Figure 2d shows the result of the two-phase separation using eqs 1 and 2. The PEG-rich phase was attracted to the inner wall and cylindrical structure of the DEX-rich phase was generated in the center. The black and red regions correspond to $\eta < 0.5$

(PEG-rich) and $\eta > 0.5$ (DEX-rich) phases, respectively. The calculations of the three- or two-phase separation qualitatively reproduce the experimental results. It should be noted that the formation of periodic patterns is a unique phenomenon only in the presence of three phases in quasi-1D confinement with the chemical affinity of the inner surface.

To date, the mechanisms of autonomous morphogenesis, as exemplified in living organisms, have been actively studied by proposing various theoretically different models. A well-known example of such mechanisms is the Turing pattern, a mathematical representation of a dissipative system characterized by reaction-diffusion kinetics. In Turing patterns, a periodic pattern emerges from the evolution of a particular wavenumber driven by activator-inhibitor dynamics. Consequently, if the influx of reactive substrates halts or undergoes significant alteration, then the spatial pattern may collapse or vanish. Conversely, lamellar or globular patterns develop during the initial stages of phase separations, where the spatial structure is marked by a certain wavenumber, for instance, in spinodal kinetics. These types of patterns can arise even within a closed system. However, the micropatterns established in the early stages typically vanish over time due to the merging of microdomains and Ostwald ripening, leading to macroscopic phase separation. Hence, achieving a stable micropattern through such phase separations is often not feasible. The present study addresses this challenge by utilizing the confining effects of a capillary, which aids in preserving the micropatterns that emerge.

In conclusion, the periodic pattern of binary droplets is produced via the phase separation of a tripolymer solution. The generated pattern is maintained, at least, for 8 h (Figure S1). The formation of this type of a pattern does not occur in the absence of quasi-1D confinement or without the specific tripolymers. These phenomena are aptly described by theoretical calculations rooted in the Cahn−Hilliard mechanism. Stable periodic structures can emerge spontaneously within a nonequilibrium closed system. This scenario could have implications for biological systems and other natural phenomena, meriting additional research.

■ ASSOCIATED CONTENT

ⓈⒾ Supporting Information

The Supporting Information is available free of charge at https://pubs.acs.org/doi/10.1021/acsmacrolett.3c00689.

> The experimental results of the periodic pattern stability for the longer time periods in a three-phase system (PEG+DEX+gelatin) within a PEG-coated glass capillary (inner diameter: 140 μm) are shown in Figure S1. Further numerical details with respect to parameters and boundary conditions (PDF)

■ AUTHOR INFORMATION

Corresponding Author

Akihisa Shioi − *Department of Chemical Engineering and Materials Science, Doshisha University, Kyoto 610-0321, Japan;* ⓘ orcid.org/0000-0002-1771-7660; Email: ashioi@mail.doshisha.ac.jp

Authors

Mayu Shono − *Department of Chemical Engineering and Materials Science, Doshisha University, Kyoto 610-0321, Japan*

Koki Aburatani − *Department of Chemical Engineering and Materials Science, Doshisha University, Kyoto 610-0321, Japan*

Miho Yanagisawa − *Komaba Institute for Science, Graduate School of Arts and Sciences, The University of Tokyo, Tokyo 153-8902, Japan; Center for Complex Systems Biology, Universal Biology Institute, The University of Tokyo, Tokyo 153-8902, Japan; Graduate School of Science, The University of Tokyo, Tokyo 113-0033, Japan;* ⓘ orcid.org/0000-0001-7872-8286

Kenichi Yoshikawa − *Faculty of Life and Medical Sciences, Doshisha University, Kyoto 610-0394, Japan; Center for Integrative Medicine and Physics, Institute for Advanced Study, Kyoto University, Kyoto 606-8501, Japan;* ⓘ orcid.org/0000-0002-2751-7136

Complete contact information is available at:
https://pubs.acs.org/10.1021/acsmacrolett.3c00689

Notes

The authors declare no competing financial interest.

■ REFERENCES

(1) Zaikin, A. A.; Schimansky-Geier, L. Spatial patterns induced by additive noise. *Phys. Rev. E* **1998**, *58* (4), 4355−4360.

(2) Löwen, H. Melting, freezing and colloidal suspensions. *Phys. Rep.* **1994**, *237* (5), 249−324.

(3) Tian, C.; Lin, L.; Zhang, L. Additive noise driven phase transitions in a predator-prey system. *Appl. Math. Model.* **2017**, *46*, 423−432.

(4) Harrington, S.; Zhang, R.; Poole, P. H.; Sciortino, F.; Stanley, H. E. Liquid-Liquid Phase Transition: Evidence from Simulations. *Phys. Rev. Lett.* **1997**, *78* (12), 2409−2412.

(5) Mishima, O.; Stanley, H. E. Decompression-induced melting of ice IV and the liquid−liquid transition in water. *Nature* **1998**, *392* (6672), 164−168.

(6) Glosli, J. N.; Ree, F. H. Liquid-Liquid Phase Transformation in Carbon. *Phys. Rev. Lett.* **1999**, *82* (23), 4659−4662.

(7) Sato, K. First-order phase transition of a vacuum and the expansion of the Universe. *Mon. Not. R. Astron. Soc.* **1981**, *195* (3), 467−479.

(8) Arndt, P. F.; Heinzel, T.; Rittenberg, V. First-Order Phase Transitions in One-Dimensional Steady States. *J. Stat. Phys.* **1998**, *90* (3), 783−815.

(9) Schmelzer, J. W.; Gokhman, A. R.; Fokin, V. M. Dynamics of first-order phase transitions in multicomponent systems: a new theoretical approach. *J. Colloid Interface Sci.* **2004**, *272* (1), 109−133.

(10) Katayama, Y.; Mizutani, T.; Utsumi, W.; Shimomura, O.; Yamakata, M.; Funakoshi, K.-i. A first-order liquid−liquid phase transition in phosphorus. *Nature* **2000**, *403* (6766), 170−173.

(11) Jamie, E. A. G.; Dullens, R. P. A.; Aarts, D. G. A. L. Spinodal decomposition of a confined colloid-polymer system. *J. Chem. Phys.* **2012**, *137* (20), 204902.

(12) Ishiguro, Y.; Tsukada, Y.; Koyama, T. Phase-field study of the spinodal decomposition rate of β phase in oxygen-added Ti−Nb alloys. *Comput. Mater. Sci.* **2020**, *174*, 109471.

(13) Xiong, H.; Qian, R.; Liu, Z.; Zhang, R.; Sun, G.; Guo, B.; Du, F.; Song, S.; Qiao, Z.-A.; Dai, S. A Polymer-Assisted Spinodal Decomposition Strategy toward Interconnected Porous Sodium Super Ionic Conductor-Structured Polyanion-Type Materials and Their

Application as a High-Power Sodium-Ion Battery Cathode. *Adv. Sci.* **2021**, *8* (11), 2004943.

(14) Das, S. K.; Roy, S.; Midya, J. Coarsening in fluid phase transitions. *C. R. Phys.* **2015**, *16* (3), 303−315.

(15) Smith, P. P. K. Spinodal decomposition in a titanomagnetite. *Am. Mineral.* **1980**, *65*, 1038−1043.

(16) Thanh, N. T. K.; Maclean, N.; Mahiddine, S. Mechanisms of Nucleation and Growth of Nanoparticles in Solution. *Chem. Rev.* **2014**, *114* (15), 7610−7630.

(17) Descamps, M.; Dudognon, E. Crystallization from the Amorphous State: Nucleation-Growth Decoupling, Polymorphism Interplay, and the Role of Interfaces. *J. Pharm. Sci.* **2014**, *103* (9), 2615−2628.

(18) Hollomon, J. H.; Fisher, J. C. Nucleation and Growth of Cell Colonies. *Science* **1950**, *111* (2888), 489−491.

(19) Mu, W.; Jia, L.; Zhou, M.; Wu, J.; Lin, Y.; Mann, S.; Qiao, Y. Superstructural ordering in self-sorting coacervate-based protocell networks. *Nature Chem.* **2023**, DOI: 10.1038/s41557-023-01356-1.

(20) Samitsu, S.; Zhang, R.; Peng, X.; Krishnan, M. R.; Fujii, Y.; Ichinose, I. Flash freezing route to mesoporous polymer nanofibre networks. *Nat. Commun.* **2013**, *4* (1), 2653.

(21) Morishige, K.; Kawano, K. Freezing and Melting of Methyl Chloride in a Single Cylindrical Pore: Anomalous Pore-Size Dependence of Phase-Transition Temperature. *J. Phys. Chem. B* **1999**, *103* (37), 7906−7910.

(22) Cheng, X.; Ullo, M. F.; Case, L. B. Reconstitution of Phase-Separated Signaling Clusters and Actin Polymerization on Supported Lipid Bilayers. *Front. Cell Dev. Biol.* **2022**, *10*, 932483.

(23) Lin, C.; He, G.; Dong, C.; Liu, H.; Xiao, G.; Liu, Y. Effect of Oil Phase Transition on Freeze/Thaw-Induced Demulsification of Water-in-Oil Emulsions. *Langmuir* **2008**, *24* (10), 5291−5298.

(24) Forrest, J. A.; Dalnoki-Veress, K. The glass transition in thin polymer films. *Adv. Colloid Interface Sci.* **2001**, *94* (1), 167−195.

(25) Lodge, T. P.; McLeish, T. C. B. Self-Concentrations and Effective Glass Transition Temperatures in Polymer Blends. *Macromol.* **2000**, *33* (14), 5278−5284.

(26) Fryer, D. S.; Peters, R. D.; Kim, E. J.; Tomaszewski, J. E.; de Pablo, J. J.; Nealey, P. F.; White, C. C.; Wu, W.-l. Dependence of the Glass Transition Temperature of Polymer Films on Interfacial Energy and Thickness. *Macromol.* **2001**, *34* (16), 5627−5634.

(27) Keddie, J. L.; Jones, R. A. L.; Cory, R. A. Interface and surface effects on the glass-transition temperature in thin polymer films. *Faraday Discuss.* **1994**, *98* (0), 219−230.

(28) Barton, B. F.; Graham, P. D.; McHugh, A. J. Dynamics of Spinodal Decomposition in Polymer Solutions near a Glass Transition. *Macromol.* **1998**, *31* (5), 1672−1679.

(29) Brostow, W.; Chiu, R.; Kalogeras, I. M.; Vassilikou-Dova, A. Prediction of glass transition temperatures: Binary blends and copolymers. *Mater. Lett.* **2008**, *62* (17−18), 3152−3155.

(30) Ash, B.; Schadler, L.; Siegel, R. Glass transition behavior of alumina/polymethylmethacrylate nanocomposites. *Mater. Lett.* **2002**, *55* (1−2), 83−87.

(31) Shono, M.; Ito, R.; Fujita, F.; Sakuta, H.; Yoshikawa, K. Emergence of uniform linearly-arranged micro-droplets entrapping DNA and living cells through water/water phase-separation. *Sci. Rep.* **2021**, *11* (1), 23570.

(32) Shono, M.; Honda, G.; Yanagisawa, M.; Yoshikawa, K.; Shioi, A. Spontaneous Formation of Uniform Cell-Sized Microgels through Water/Water Phase Separation. *Small* **2023**, *19* (38), 2302193.

(33) Bai, Q.; Chen, X.; Chen, J.; Liu, Z.; Lin, Y.-n.; Yang, S.; Liang, D. Morphology and Dynamics of Coexisting Phases in Coacervate Solely Controlled by Crowded Environment. *ACS Macro Lett.* **2022**, *11* (9), 1107−1111.

(34) Lu, T.; Spruijt, E. Multiphase Complex Coacervate Droplets. *J. Am. Chem. Soc.* **2020**, *142* (6), 2905−2914.

(35) Mountain, G. A.; Keating, C. D. Formation of Multiphase Complex Coacervates and Partitioning of Biomolecules within them. *Biomacromol* **2020**, *21* (2), 630−640.

(36) Karoui, H.; Seck, M. J.; Martin, N. Self-programmed enzyme phase separation and multiphase coacervate droplet organization. *Chem. Sci.* **2021**, *12* (8), 2794−2802.

(37) Bai, Q.; Liu, Z.; Chen, J.; Liang, D. Crowded Environment Regulates the Coacervation of Biopolymers via Nonspecific Interactions. *Biomacromol* **2023**, *24* (1), 283−293.

(38) Guzowski, J.; Korczyk, P. M.; Jakiela, S.; Garstecki, P. The structure and stability of multiple micro-droplets. *Soft Matter* **2012**, *8* (27), 7269−7278.

(39) Turing, A. M. The chemical basis of morphogenesis. *Philos. Trans. R. Soc. B* **1952**, *237* (641), 37−72.

(40) Barrio, R. A.; Varea, C.; Aragón, J. L.; Maini, P. K. A Two-dimensional Numerical Study of Spatial Pattern Formation in Interacting Turing Systems. *Bull. Math. Biol.* **1999**, *61* (3), 483−505.

(41) Kéfi, S.; Eppinga, M. B.; de Ruiter, P. C.; Rietkerk, M. Bistability and regular spatial patterns in arid ecosystems. *Theor. Ecol.* **2010**, *3* (4), 257−269.

(42) Talukdar, D.; Dutta, K. Transition of Spatial Patterns in an Interacting Turing System. *J. Stat. Phys.* **2019**, *174* (2), 351−364.

(43) Tsumoto, K.; Arai, M.; Nakatani, N.; Watanabe, S.; Yoshikawa, K. Does DNA Exert an Active Role in Generating Cell-Sized Spheres in an Aqueous Solution with a Crowding Binary Polymer? *Life* **2015**, *5* (1), 459−466.

(44) Ma, C.; Chen, X. D.; Kong, Y.-q.; Che, L. Phase Diagram of Aqueous Two-Phase System (ATPS) Composed of Polyethylene Glycol (PEG) and Gelatin. *Adv. Materials Res.* **2012**, *554−556*, 286−294.

(45) Yanagisawa, M.; Nigorikawa, S.; Sakaue, T.; Fujiwara, K.; Tokita, M. Multiple patterns of polymer gels in microspheres due to the interplay among phase separation, wetting, and gelation. *Proc. Natl. Acad. Sci. U. S. A.* **2014**, *111* (45), 15894−15899.

(46) Butler, M. F.; Heppenstall-Butler, M. Phase separation in gelatin/dextran and gelatin/maltodextrin mixtures. *Food Hydrocolloids* **2003**, *17* (6), 815−830.